Elementary Processes in Photoinduced Proton Transfers in 2-Hydroxy-1-(*N*-morpholinomethyl)naphthalene and 7-Hydroxy-8-(*N*-morpholinomethyl)quinoline in Liquid Solutions

Erik J. A. de Bekker, Audrius Pugzlys, and Cyril A. G. O. Varma*

Leiden Institute of Chemistry, Leiden University, Gorlaeus Laboratories, P.O. Box 9502, 2300 RA Leiden, The Netherlands

Received: July 19, 2000; In Final Form: October 19, 2000

The evolution of a primary excited electronic state of 2-hydroxy-1-(*N*-morpholinomethyl)naphthalene (HMMN) and 7-hydroxy-8-(*N*-morpholinomethyl)quinoline (HMMQ) in liquid solutions has been followed with a time resolution of 200 fs by detecting the emerging transient UV−visible absorptions and stimulated emissions. The primary state lies about 7000 cm^{-1} above the state S_1. The spectral changes in the case of HMMN in *n*-hexane are attributed to vibrational relaxation, because intramolecular proton transfer (i.e., formation of the excited zwitterionic form *Z**) does not take place and effects due to dielectric polarization of the solvent could be ruled out. A similar vibrational relaxation has been observed in the case of HMMN in tetrahydrofurane. The *Z** state of HMMN emerges in tetrahydrofurane, but only from a complex {*E**,*S*} of the excited enol form (*E**) and a solvent molecule (*S*) and certainly not from the vibrationless S_1 state of *E**. The transferable proton in {*E**,*S*} is simultaneously involved in an intramolecular and an intermolecular H-bond. HMMN behaves in a similar fashion as in tetrahydrofurane, when the former is dissolved in 1,4-dioxane. In the case of HMMN in acetonitrile, the evolution of triplet states $^3\{Z^*,S\}$ can be seen in addition to a quasistationary singlet state $^1\{Z^*,S\}_1$. The intersystem crossing from the singlet into the triplet manifold of states proceeds from $^1\{Z^*,S\}$ states above the vibrationless state $^1\{Z^*,S\}_1$. The triplet state formation is attributed to the weaker intermolecular H-bond involved in the complex {*Z**,*S*} when $S = CH_3CN$. Dielectric polarization of the solvent is of no significance in promoting the intramolecular proton transfer compared to the specific solute−solvent interaction in the complex {*E**,*S*}. The protonated morpholino group in the *Z*-* form of HMMN is kept fixed by an intramolecular H-bond in all the cases. In the case of HMMQ, only its solution in tetrahydrofurane has been studied. The rate constant for the conversion of the *Z** form of HMMQ into the excited keto (*K**) form has been determined, as well as the rate constant for the relaxation of the latter into the ground-state keto form (*K*). The rate constant for the conversion of the form *K* of HMMQ into the ground-state enol form (through rotational Brownian motion of the protonated morpholino group) has also been determined. Spectral broadening arising from the motion of the protonated morpholino group in the *Z** form of HMMQ has been observed in accordance with previous simulations.

Introduction

Time-resolved spectroscopic studies of photoinduced proton transfer processes have revealed several aspects of the mechanisms involved in liquid-state intramolecular proton transfers over relatively short distances. The mechanisms are quite complex and involve active participation of the solvent and proton tunneling through hydrogen bonds, as, for instance, in the case of photoexcited 7-azaindole and the ground state of the keto tautomer of 7-hydroxyquinoline (7-HQ) dissolved in alcohols.[1,2] The two cases mentioned are examples of several cases in which proton tunneling through H-bonds became evident from the observed temperature-independent kinetic isotope effect on the rate constant for the proton transfer. Long-distance proton transfers are expected to be even more complex than in the case of short distances, because the proton, besides having to detach from the source and attach to the target, has to be transported on a carrier over a large distance through the bulk of the medium.

The molecule 7-hydroxy-8-(*N*-morpholinomethyl)naphthalene (HMMN) may exhibit a photoinduced proton transfer from the OH group to the N atom in the morpholino ring, resulting in a zwitterionic form.[3] The photosensitive part of HMMN is a 2-hydroxynaphthyl group, whose OH group becomes a stronger proton donor than in the ground state when it gets into an excited electronic singlet state.[4] The morpholino group may then accept the proton, but it does so only when HMMN is dissolved in a polar solvent. It is not yet clear how the polar solvent assists in the transfer of the proton within photoexcited HMMN. Two possibilities are worth considering, namely formation of a complex either between a solvent molecule and the excited solute or through interaction of the latter with the electric field arising from the dielectric polarization it induces in the solvent. The present study aims at eliminating one of these possibilities and at finding similarities with the known behavior of the photoexcited enol form of HMMQ.

Replacing the CH group in position 8 of the ring system of 2-hydroxynaphthol yields the molecule 7-hydroxyquinoline. The same substitution converts HMMN into the molecule 7-hydroxy-8-(*N*-morpholinomethyl)quinoline (HMMQ). This molecule was designed[5] to serve as a model offering the possibility for in-depth experimental studies of long-distance proton transfer in

* To whom all correspondence should be addressed.

10.1021/jp002581k CCC: $20.00
Published on Web 12/21/2000

systems in which the source and the target are not connected, as, e.g., in an alpha-helix peptide structure,[6] by a chain of hydrogen bonds.

Adiabatic excited state intramolecular proton transfer (ESIPT) from the OH group to the morpholino's N atom can be observed in the case of HMMN only when it is dissolved in a polar solvent,[3,5] and in the case of HMMQ when it is dissolved in either a nonpolar or a polar solvent.[5,7−12] In the case of solutions of HMMQ in polar solvents or in 1,4-dioxane, the first ESIPT step is followed by rotational Brownian motion of the protonated side group, which enables delivery of the proton at the N atom in the quinoline ring and results in formation of the excited keto form of HMMQ. The fluorescence spectrum of HMMN in an alkane consists of a single band, that arises from the excited enol form, with its maximum at 363 nm. The fluorescence spectrum of the solution of HMMN in methanol or acetonitrile is dominated by a band, arising from the 2-naphtholate ion in HMMN formed adiabatically through ESIPT. This band has its maximum at 417 and 422 nm in the cases of HMMN in methanol and acetonitrile, respectively.[3,5] The fluorescence spectrum of HMMQ in alkanes shows a band with maximum at 417 nm with a shoulder at 380 nm. The main band and the shoulder arise from the excited zwitterion, formed adiabatically through ESIPT, and from the excited enol form, respectively.[5] A third band appears at the red side in the fluorescence spectrum of HMMQ when it is dissolved in polar solvents or in 1,4-dioxane. This band arises from the excited keto form of HMMQ, which is formed adiabatically from the excited zwitterion.[5,10,11]

Previous studies revealed how solvents act in the catalysis of the multistep, photoinduced enol−keto tautomerization of HMMQ.[5,7−12] These studies provide reaction schemes (Figure 1) and other useful information concerning the conversion process. Two forms of HMMQ are in the ground state when the solvent contains proton acceptors (*S*), namely a bare form with an intramolecular H-bond and a complex in which the proton in the intramolecular H-bond is also H-bonded to *S*. It has been concluded that only the latter exhibits photoinduced enol−keto tautomerization.[12] It seems that both forms are converted to a zwitterionic form by proton tunneling, which proceeds only before vibrational relaxation of the excess energy deposited with the excitation.[12] It has been suggested that part of the excess energy in the complex with *S* is used to break the intramolecular H-bond and to set the protonated side group into rotational Brownian motion. However, the processes involved in the detachment of the proton from the OH group in the excited state of HMMQ could not be observed directly with the time resolution of 5 ps available at the time. The ground-state reverse tautomerization leading from the ground-state keto form to the original enol form could not be observed in the case of HMMQ, although this process could be followed in great detail on a microsecond and submicrosecond time scale in the case of the photogenerated keto tautomer of 7-HQ in alcohols.[2] Here we report a time-resolved spectroscopic study with improved time resolution intended to verify the suggestion concerning the requirement of excess energy for detaching the proton from its initial site. UV-laser pulses of about 200 fs duration have been used to generate the primary excited state of HMMN and HMMQ with energy exceeding that of their vibrationless lowest excited singlet state. The evolution of the primary excited singlet state has been monitored by means of time-resolved absorption spectroscopy at a number of selected wavelengths in the visible region of the spectrum. The proton transfer succeeding the optical excitation of HMMN and HMMQ was too fast to be detected in real time even with the improved time resolution, but relevant information could be acquired in the case of HMMN. Similar information could not be obtained in the case of HMMQ, because the transient spectral bands appearing in successive stages of the tautomerization process are severely broadened and overlapping. The merit of the HMMQ study is that the time scale of the ground-state reverse tautomerization of HMMQ could be revealed.

We first present the study concerning the solution of HMMN in *n*-hexane because ESIPT does not take place in this case. We then present the study of the solutions of HMMN in tetrahydrofurane and in 1,4-dioxane because in these cases the stationary fluorescence reveals substantial contributions from both the excited enol form and the excited zwitterionic form. Subsequently, we consider the solution of HMMN in acetonitrile because its stationary fluorescence spectrum is dominated by the excited zwitterionic form. Finally, we discuss the study of the solution of HMMQ in tetrahydrofurane.

Experimental Section

2-Hydroxy-1-(*N*-morpholinomethyl)naphthalene (HMMN) and 7-hydroxy,8-(*N*-morpholinomethyl)quinoline (HMMQ) were prepared and purified as described previously.[3,5] *n*-Hexane, tetrahydrofurane, and acetonitrile were of spectroscopic quality and were used as delivered. Sodium was added to the solvent 1,4-dioxane, which was then boiled in a refluxing apparatus for several hours until it had to be used. It was then distilled before use. The solvents used did not show any (linear) absorption in the UV and visible wavelength range covered. The solutions were not deoxygenated. Absorption spectra were recorded on a Perkin-Elmer Lambda 2 UV−vis spectrophotometer.

In the pump−probe studies a laser system has been used which consists of a c.w. modelocked Titanium Sapphire laser oscillator (Coherent, model MIRA) followed by a regenerative laser amplifier operating at 1 kHz repetition rate (B. M. Industries, model ALPHA 1000). Optical pulses generated as the third harmonic of the amplified laser pulses were used for the primary excitation of the sample. These pulses in the pump beam had a total energy (E_P) of about 500 nJ and a wavelength of 266 nm. The main 266-nm laser beam was split into a reference pump beam, used to determine E_P, and an actual pump beam. Wavelength-tunable optical parametric generators (OPGs) and amplifiers (OPAs) were pumped by pulses emerging from the BMI ALPHA system to generate pulses for probing the evolution of the excited sample. The beam emerging from the OPG/OPA system (B.M. Industries) was also split to obtain a reference probe beam and an actual probe beam. The probe beam was polarized at magic angle (54.7°) with respect to the polarization of the pump beam, and its intensity may be considered too low to excite detectable two-photon fluorescence of the solutions. The pump and probe beams were nearly collinear; they entered the cylindrical sample cell (1 mm path length; 50 mm diameter) perpendicular to its windows and were off axis with respect to the cylinder axis, while the cell rotated at high speed along the latter axis. In this manner, effects of sample decomposition could be avoided, because each pump−probe pulse pair investigated a fresh portion of the sample. The absorption spectra of the samples showed no change after completion of the measurement. The induced change in optical absorbance, $\Delta A(\lambda,t)$, was determined from the attenuation of each probe pulse transmitted through the sample and detected with photodiodes responding linearly. The time (t) elapsed between primary excitation and probing was varied by means

of an optical delay line. In this manner the absorbance change at fixed wavelength (λ) is obtained as a function of time, $\Delta A_\lambda(t)$. The value of $\Delta A_\lambda(t)$ at fixed t was averaged over a sufficiently large number of pump−probe pulse pairs to achieve a good signal-to-noise ratio. To compare changes in absorbance at different wavelengths, $\Delta A_\lambda(t)$ was normalized with respect to E_P. The optical alignment of pump, probe, and reference beams was kept fixed in series of recordings which were compared, and it was verified that E_P remained constant while t was scanned. The probing covered the wavelength region between 460 and 807 nm. An indication of spectral changes with time was obtained by plotting $\Delta A_t(\lambda)$, which represents $\Delta A(\lambda,t)$ at the discrete λ's for various specified times. Two-color, two-photon absorption by neat liquid 1,4-dioxane was used to determine the cross correlation between pump and probe pulse.[13] Time $t = 0$ was defined as the time when the maximum in the two-photon absorption appears. The width of the probe pulses depended on the wavelength, but the cross correlation function just mentioned had always a width of less than 450 fs, which means that the width of the probe pulses was less than 400 fs.

The lifetime of the fully relaxed fluorescent state was determined either by correcting published values for deoxygenated solutions for quenching by oxygen, or by detecting the time dependence of the fluorescence with a streak camera after excitation with a 4 ps/300 nm laser pulse. The fluorescence quenching by oxygen has been determined experimentally, when necessary, by comparison of the fluorescence intensity prior and after deoxygenation of the solution.

The neat solvents 1,4-dioxane and tetrahydrofurane exhibit two-photon absorption (TPA) consisting of simultaneous absorption of a photon from the pump and probe beams. The quantity $\Delta A_\lambda(t)$ is determined from the intensity change of the probe beam in this TPA process, and its shape is taken to represent the shape of the response function $R(t)$ of the pump−probe detection system. The experimentally determined function $\Delta A_\lambda(t)$ of the photoexcited solution is the superposition of $R_\lambda(t)$ and the convolution $S_\lambda(t)$ of $R_\lambda(t)$ and the absorbance change $\Delta A_{\lambda m}(t)$ arising from absorption by transient molecular species. The function $S_\lambda(t)$ was simulated as the convolution of $R(t)$ and a sum of exponential functions of t, with the latter representing $\Delta A_{\lambda m}(t)$. The time resolution achieved in this manner is expected to be equal to half the width of the probe pulse, i.e., not worse than 200 fs.

The optical delay line used offers a maximum delay of 1 ns. The delay was extended, when needed, to several nanoseconds by displacing the delay line along the direction of the incoming probe beam to increase its path length without disturbing the alignment. Pinholes were used to define the alignment.

Results and Discussion

1. Solution of HMMN in *n*-Hexane. ***1.a. Features of the Transient Absorption Spectrum.*** HMMN is photochemically a simpler system than HMMQ. Because solutions of HMMN in *n*-hexane exhibit only fluorescence from the enol form, their photoinduced transient absorptions, $\Delta A_\lambda(t)$, may be attributed to optical transitions from excited states of the enol form. Excitation of 266 nm with the laser pulse prepares molecules in the second excited singlet state S_2. Their excess energy above the vibrationless lowest excited singlet state S_1, ΔE_d, is subsequently dissipated by the environment, presumably after electronic relaxation into S_1. In the case of HMMN in *n*-hexane, ΔE_d is estimated to be about 7740 cm^{-1}.

The features of $\Delta A_t(\lambda)$ are shown in Figure 2 for various values of t. The pump process with the UV laser pulse proceeds

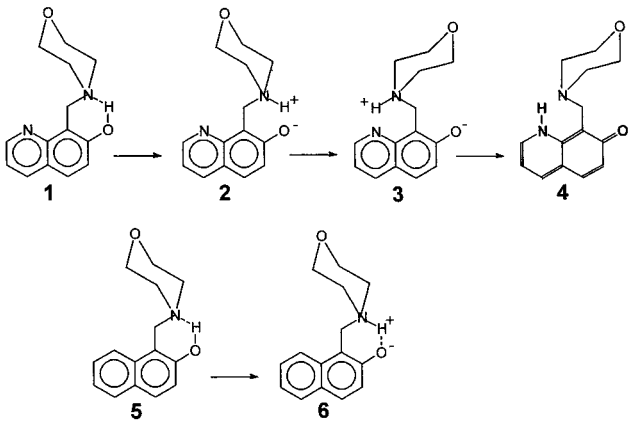

Figure 1. Structures of various forms of HMMQ and HMMN: **1**, enol forms *E* and *E** of HMMQ with *intra*molecular H-bond; **2**, *zwitterionic* forms *Z* and *Z** of HMMQ immediately after *intra*molecular proton transfer in *E* and *E**, respectively; **3**, *zwitterionic* forms *Z* and *Z** of HMMQ after a 180° rotation of the morpholino group; **4**, keto forms *K* and *K** of HMMQ; **5**, enol forms *E* and *E** of HMMN with *intra*molecular H-bond; **6**, *zwitterionic* forms *Z* and *Z** of HMMN maintaining an *intra*molecular H-bond after *intra*molecular proton transfer in *E* and *E**, respectively.

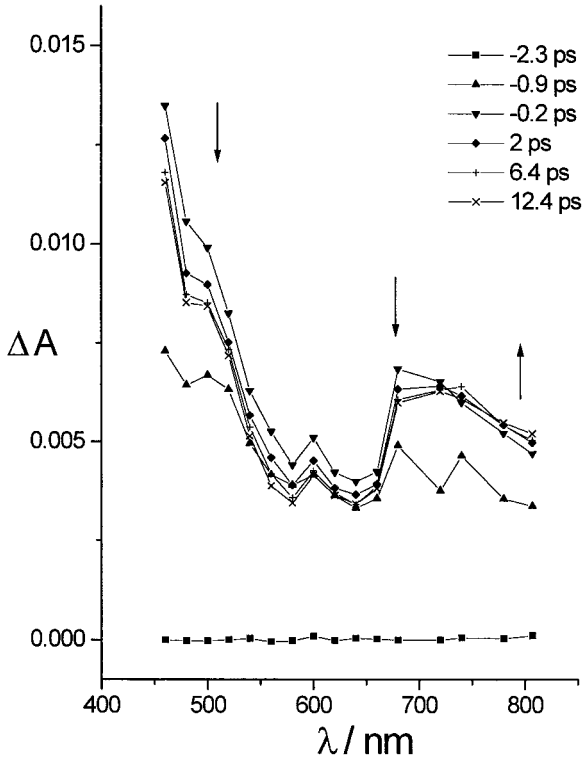

Figure 2. Evolution of the transient absorption spectrum of the solution of HMMN in *n*-hexane.

in the period before the time marked in this figure as $t = -0.2$ ps. The features of $\Delta A_t(\lambda)$ seem to consist of the red edge of a band, ΔA_B, in the blue part and a band, ΔA_R, in the red part of the spectrum. Relatively large magnitudes of $\Delta A_t(\lambda)$ can be observed (Figure 2) at 480, 680, and 807 nm. The initial absorptions below 680 nm diminish in time, while absorptions above this wavelength are increasing. Roughly speaking, the shape of the band ΔA_R changes slightly after termination of the excitation process. The shape of the red edge of ΔA_B changes during the excitation process, but later, its evolution may be considered to indicate either a uniform blueshift or an attenuation of the band. In principle, solvent reorganization around the excited solute may cause a time-dependent spectral shift of the

transient absorption bands and therefore contribute also to the features of the fast kinetics. The effect could arise only from the anisotropy of the polarizability, of *n*-hexane. In the case of an isotropic polarizability, the effect would vanish. It is worthwhile to estimate an order of magnitude of a band shift, $\Delta\sigma$, arising from coupling of the reaction field, **R**, of the solvent to the molecular dipoles, $\boldsymbol{\mu}_i$ and $\boldsymbol{\mu}_f$, of the initial and final electronic state involved in the transition. In the case of the nonpolar solvent *n*-hexane, the shift $\Delta\sigma$, arising from Onsager's field **R**, is

$$\Delta\sigma = \frac{1}{hca^3}\left(\frac{n^2-1}{n^2+2}\right)(\mu_i^2 - \mu_f^2) \qquad (1)$$

where *h*, *c*, *a*, and *n* are Planck's constant, the velocity of light, the cavity radius for the solute, and the refractive index of the solvent, respectively. Because both μ_i and μ_f have finite values and are not expected to exceed a magnitude of, say, 25 D units, the value of $\Delta\sigma$ is much less than 1 cm^{-1} when *a* is as small as 3 Å. The apparent shift of ΔA_B after completion of the excitation process is about 700 cm^{-1} and cannot arise from *dipole−reaction field* interaction. The modification of the shape of ΔA_B during the excitation process can be attributed to electronic relaxation into the state S_1 while the excitation is going on, whereby the energy ΔE_d is being redistributed among vibrational modes of the state S_1. The subsequent change in the appearance of ΔA_B may be explained as a uniform attenuation by assuming that all molecules in the state S_1 have their vibrational modes unexcited, with the exception of a single mode. The excess energy in the state S_1 is released and dissipated by the solvent, presumably in single quantum jumps. Denote the excited vibrational mode by Q_B and its fundamental wavenumber and *n*th wave function in the *j*th electronic state by σ_{jB} and Ω_{jBn} respectively, where *j* refers to either the state *i* or *f* mentioned above. Consider transitions in which Ω_{iBn} changes into Ω_{fBm}. If $\sigma_{iB} \approx \sigma_{fB}$, then the simultaneous substitution of, e.g., Ω_{iBn} by Ω_{iBn-1} and Ω_{fBm} by Ω_{fBm-1} leaves the transition energy nearly unchanged, but modifies the intensity by a factor $R_{nn-1} = \langle\Omega_{iBn} \mid \Omega_{fBm}\rangle^2/\langle\Omega_{iBn-1} \mid \Omega_{fBm-1}\rangle^2$ over a spectral range of about σ_B cm^{-1}. When several vibrational modes are excited in the S_1 population, the spectral changes in the course of the vibrational relaxation become very complex and are not expected to resemble those observed in ΔA_B. The evolution of ΔA_R is slightly different from the development of ΔA_B after termination of the pump process. At the very red edge, the intensity is increasing slightly as time progresses. This can be attributed to the difference between the final electronic states of the two electronic transitions. The displacement of the mode Q_B may be quite different for the latter two states, and the frequency of the mode may change also. A maximum may be encountered in the Franck−Condon factor as the vibrational relaxation proceeds. At any rate within a selected time window, the bands ΔA_B and ΔA_R must reveal the same kinetics.

1.b. Time Dependence of the Transient Optical Absorptions. Figure 3 shows the time dependence of $\Delta A_\lambda(t)$ at 480, 680, and 807 nm in the case of a solution of HMMN in *n*-hexane. Stimulated emission contributes to the magnitude of $\Delta A_\lambda(t)$ between 460 and 500 nm. Figure 3 reveals clearly that fast processes are running in the first 10 picoseconds; these fast processes are then followed by a rather slow one. This slow process can be identified with the decay of the fully relaxed lowest excited singlet state of the enol form of HMMN. Its decay rate constant will be referred to as k_L, and its magnitude has been determined experimentally to be 0.36×10^9 s^{-1}. At least three exponential functions are required to reproduce the

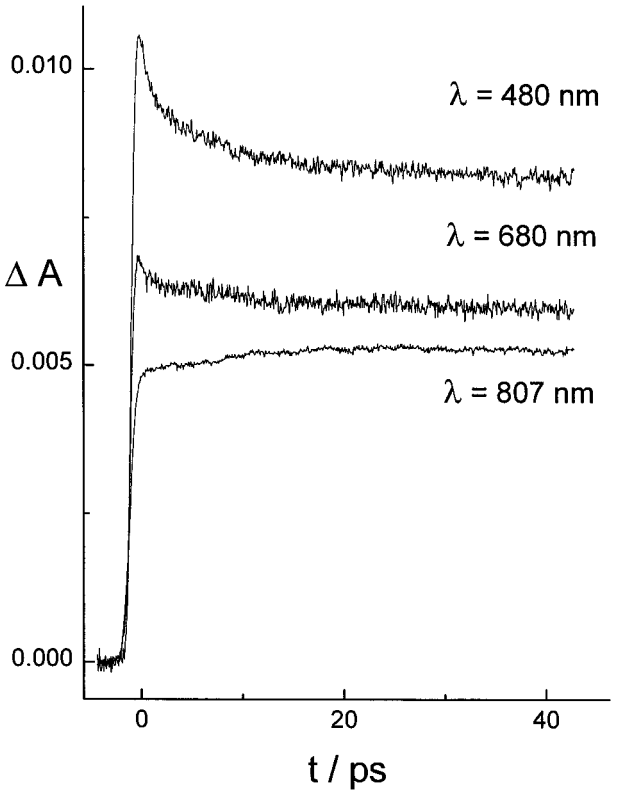

Figure 3. Time dependence of the transient absorptions of the solution of HMMN in *n*-hexane at 480, 680, and 807 nm.

observed time profiles $\Delta A_\lambda(t)$ at the various wavelengths. They have been expressed as

$$\Delta A\,(t) = \sum_{j=1}^{m} a_j \exp(-k_j t) + a_L \exp(-k_L t)$$

$$\text{with } m = 1, 2, \text{ or } 3 \qquad (2)$$

where the first terms account for the fast processes and the last term represents the decay of the relaxed excited enol form in its state S_1. The ratio a_j/k_j can be considered to be a measure of the weight of the *j*th component in the representation. Table 1 lists the parameters in the representation of $\Delta A_\lambda(t)$ at a number of wavelengths.

Table 1 shows that the fast kinetics varies with wavelength and that not more than two exponentials are required to reproduce it. Note: $k_2 > k_1$. The fast components in $\Delta A_\lambda(t)$ correspond to a decay (positive a_j) between 460 and 700 nm and a growth (negative a_j) of $\Delta A_\lambda(t)$ above 720 nm. The values of the parameters in the representation of the recorded signals $\Delta A_{720}(t)$ and $\Delta A_{740}(t)$ are not very significant, because the signals are nearly constant in the time range covered after termination of the laser excitation pulse. However, the signs of these parameters are trustworthy. The rate constants k_1 and k_2 needed to represent the signals $\Delta A_{460}(t)$ and $\Delta A_{480}(t)$ are significantly larger than those for the other wavelengths. This can be taken as evidence that the state S_2 contributes also to the latter signals, because the other wavelengths k_1 and k_2 do not vary much. This observation is in accordance with the suggestion made above, that the bands ΔA_B and ΔA_R must reveal the same kinetics.

A simple mother−daughter relation between the primary excited-state population and the fully relaxed excited-state population would need only two exponential functions to fit $\Delta A_{\lambda m}(t)$. Taking into account that vibrational substructure is not resolved, that each sublevel carries a different transition

TABLE 1: Kinetic Parameters for HMMN in *n*-Hexane

λ [nm]	$10^3\, a_1$	k_1 [10^{12} s^{-1}]	$10^3\, a_2$	k_2 [10^{12} s^{-1}]	$10^3\, a_L$	k_L [10^9 s^{-1}]
460	1.38 ± 0.1	0.10 ± 0.01	1.7 ± 0.1	0.49 ± 0.06	11.24 ± 0.01	0.36 ± 0
480	1.43 ± 0.05	0.140 ± 0.006	3.35 ± 0.2	1.44 ± 0.1	8.34 ± 0.007	0.36 ± 0
500	0.56 ± 0.01	0.045 ± 0.005	2.09 ± 0.04	0.61 ± 0.02	8.11 ± 0.02	0.36 ± 0
520	0.46 ± 0.04	0.079 ± 0.009	1.3 ± 0.04	0.59 ± 0.04	6.97 ± 0.009	0.36 ± 0
540	0.73 ± 0.03	0.058 ± 0.006	1.43 ± 0.05	0.56 ± 0.04	4.84 ± 0.02	0.36 ± 0
560	1.13 ± 0.02	0.072 ± 0.003	1.6 ± 0.04	0.71 ± 0.04	4.94 ± 0.01	0.36 ± 0
580	1.22 ± 0.03	0.078 ± 0.004	1.6 ± 0.06	0.75 ± 0.06	4.26 ± 0.01	0.36 ± 0
600	0.66 ± 0.03	0.077 ± 0.005	1.04 ± 0.04	0.63 ± 0.05	3.91 ± 0.007	0.36 ± 0
620	0.51 ± 0.03	0.061 ± 0.01	1.01 ± 0.06	0.63 ± 0.08	4.70 ± 0.02	0.36 ± 0
640	0.48 ± 0.02	0.051 ± 0.007	0.91 ± 0.03	0.51 ± 0.04	4.53 ± 0.02	0.36 ± 0
660	0.28 ± 0.06	0.12 ± 0.03	0.67 ± 0.08	0.8 ± 0.2	5.05 ± 0.008	0.36 ± 0
680	0.60 ± 0.08	0.13 ± 0.02	0.7 ± 0.1	1.0 ± 0.4	7.89 ± 0.01	0.36 ± 0
720	too weak	too weak	too weak	too weak	too weak	too weak
740	−0.30 ± 0.03	0.82 ± 0.02			6.38 ± 0.02	0.36 ± 0
780	−0.63 ± 0.03	0.086 ± 0.005	−5.5 ± 0.01	4.1 ± 0.9	5.8 ± 0.01	0.36 ± 0
807	−0.59 ± 0.15	0.107 ± 0.004	−5.01 ± 0.07	6 ± 4	5.37 ± 0.007	0.36 ± 0

probability in the optical absorption, and that the relaxation rate constant varies among the sublevels, the kinetics of the fast process is not expected to be uniform as a function of wavelength, and that it can be represented by a sum of merely a few exponential functions. The need for only two exponential functions to represent the fast kinetics can be considered evidence that at the end of the excitation process, most of the excess energy ΔE_d is stored in about two quanta of a single vibrational mode, as suggested above. The excitation pulse is populating the state S_2, and there is spectral evidence for electronic relaxation from S_2 to S_1 during the excitation process. For these reasons, it is reasonable to assume that at the end of the pulse the excited-state population consists predominantly of enol-type solutes in the state S_1, with the excess energy of about 7000 cm^{-1} stored in a high-frequency accepting mode Q_a like a C−H or O−H stretching vibration. This assumption implies that redistribution of vibrational energy in S_2 is causing conversion of the whole S_2 population into an S_1 population through mode Q_a only. If the fundamental wavenumber σ_a of Q_a satisfies 2000 cm^{-1} $\leq \sigma_a \leq$ 3000 cm^{-1}, then Q_a does not get excited with more than 3 quanta. Of course, the mode Q_B mentioned above has to be identified with the mode Q_a.

2. Solution of HMMN in Tetrahydrofurane. ***2.a. Features of the Transient Absorption Spectrum.*** The induced absorptions $\Delta A_t(\lambda)$ of the solution of HMMN in tetrahydrofurane are shown in Figure 4. The excitation process precedes the time marked as $t = 0.2$ ps in this figure. Within this period, features of the transient absorption spectrum can already be seen over the whole wavelength region at $t = -0.6$ ps. In the region $\lambda < 600$ nm, the maximum magnitude of $\Delta A_t(\lambda)$ is observed at $t = -0.2$ ps. For -1.3 ps $\leq t \leq -0.2$ ps (period 1), the spectral changes can be attributed to relaxation of the states prepared directly by the pump pulse, as in the case of HMMN in *n*-hexane. The magnitude of $\Delta A_t(\lambda)$ below 520 nm drops slightly for $-0.2 < t \leq 0$ ps (period 2). This observation is evidence that the TPA contribution by the solvent is absent after $t = 0$ ps, because in the subsequent interval $0 < t \leq 0.2$ ps (period 3), the magnitude of $\Delta A_t(\lambda)$ in the region $480 \leq \lambda < 560$ nm, ΔA_B, drops uniformly, similarly to the change of ΔA_B in the case of HMMN in *n*-hexane. Therefore, the changes in ΔA_B in period 3 in the present case can also be attributed to vibrational relaxation of the enol form of HMMN in the state S_1. Faint features of a band around 640 nm, ΔA_Z, can be observed as early as $t = -0.6$ ps, i.e., during the pump process; these features develop into an intense band later. Because a similar band does not appear in the case of HMMN in *n*-hexane, the intense band can be attributed to absorption by the excited zwitterionic form Z^* of HMMN, formed adiabatically from its excited enol form E^* or from a complex involving the latter. The band ΔA_Z has nearly reached its maximum intensity at the end of period 3, and its intensity grows just a bit more between $0.2 < t \leq 22$ ps (period 4). This means that the excited zwitterion of HMMN is not formed predominantly from E^* in the state S_1.

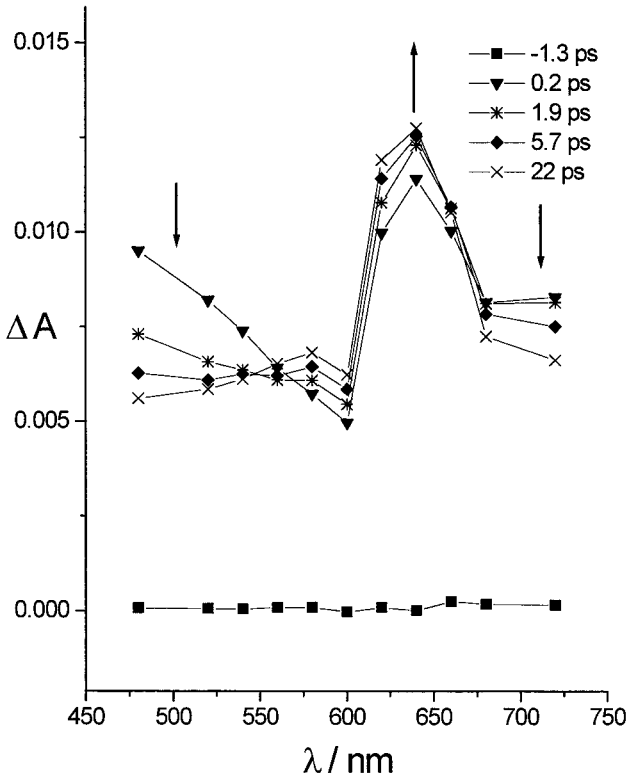

Figure 4. Evolution of the transient absorption spectrum of the solution of HMMN in tetrahydrofurane.

2.b. Time Dependence of the Transient Optical Absorptions. Figure 5 shows the time dependence of $\Delta A_\lambda(t)$ at 480, 640, and 720 nm. Two-photon absorption by the solvent clearly contributes to $\Delta A_\lambda(t)$ at 480 nm, but not at 640 and 720 nm. Since E^* and Z^* are being interconverted rapidly compared to their decay,[5] they decay collectively. The rate constant for their collective decay, k_L, has been obtained from the decay of the fluorescence and entered as a fixed-rate constant k_L in the representation of $\Delta A_\lambda(t)$ given in eq 2.

An example of such a representation is presented in Figure 6. The parameters in this representation are listed in Table 2 for all probe wavelengths. Note again: $k_2 > k_1$.The rate

TABLE 2: Kinetic Parameters for HMMN in Tetrahydrofurane

λ [nm]	$10^3\, a_1$	k_1 [10^{12} s^{-1}]	$10^3\, a_2$	k_2 [10^{12} s^{-1}]	$10^3\, a_L$	k_L [10^9 s^{-1}]
480	1.47 ± 0.06	0.07 ± 0.01	4.6 ± 0.2	0.98 ± 0.07	5.3 ± 0.03	0.31 ± 0
520	0.71 ± 0.06	0.07 ± 0.01	2.0 ± 0.1	0.69 ± 0.08	5.6 ± 0.03	0.31 ± 0
540	0.16 ± 0.03	0.05 ± 0.03	1.6 ± 0.2	1.1 ± 0.1	6.07 ± 0.04	0.31 ± 0
560	−0.44 ± 0.03	0.07 ± 0.01			6.56 ± 0.02	0.31 ± 0
580	−1.08 ± 0.01	0.13 ± 0.01			6.95 ± 0.01	0.31 ± 0
600	−1.36 ± 0.02	0.17 ± 0.01			6.39 ± 0.01	0.31 ± 0
620	−1.71 ± 0.05	0.19 ± 0.01			11.92 ± 0.01	0.31 ± 0
640	−0.97 ± 0.19	0.40 ± 0.06	−11 ± 15	4.2 ± 0.3	12.73 ± 0.01	0.31 ± 0
660	0.80 ± 0.09	0.04 ± 0.02	−0.9 ± 0.3	0.80 ± 0.41	10.1 ± 0.1	0.31 ± 0
680	1.35 ± 0.02	0.09 ± 0.01			7.15 ± 0.01	0.31 ± 0
720	2.05 ± 0.03	0.13 ± 0.01			6.75 ± 0.01	0.31 ± 0

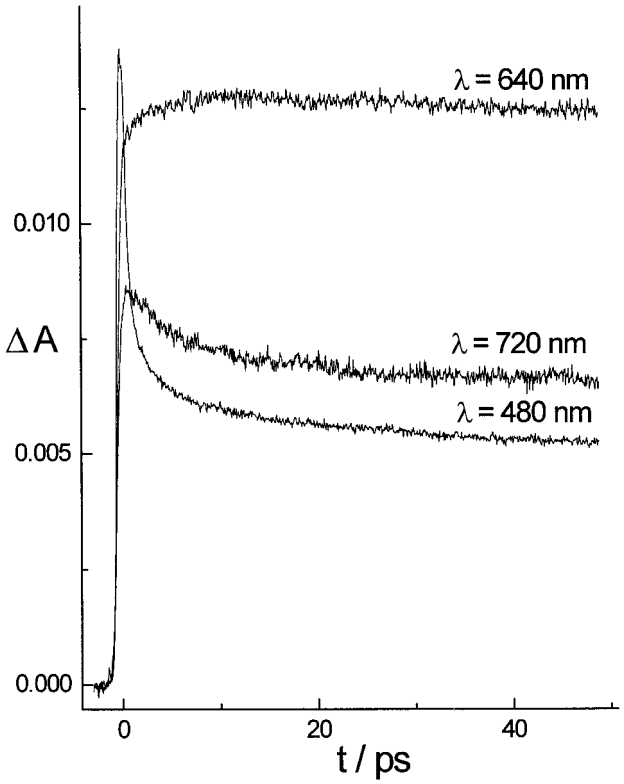

Figure 5. Time dependence of the transient absorptions of the solution of HMMN in tetrahydrofurane at 480, 640, and 720 nm.

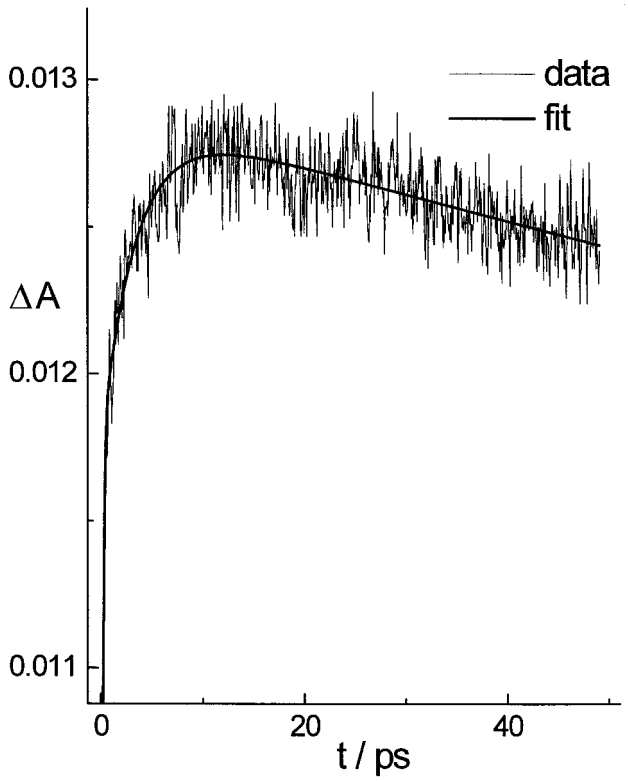

Figure 6. Experimental and fitted time dependence of the transient absorption of the solution of HMMN in tetrahydrofurane at 640 nm.

constants k_1 and k_2 for $\lambda = 640$ nm and $\lambda = 660$ nm will be ignored in the discussion, because they are not very accurate, apparently as the consequence of overlap of a decaying and a growing band which have about equal rate constants and weight in the representation. The values of k_2 in the range $480 \leq \lambda \leq 540$ nm (band ΔA_B) do not differ much from those obtained in the band ΔA_B in the case of HMMN in *n*-hexane. Therefore, the band ΔA_B can also be attributed in the present case to absorptions by both E^* in the state S_1, carrying vibrational excitation, and by the initially prepared E^* in the state S_2. The changes in the band ΔA_B with time can also be attributed in this case to electronic relaxation of S_2 followed by vibrational relaxation of the emerging state S_1.

The component in the kinetics with rate constant k_2 vanishes outside the band ΔA_B, unlike the case of HMMN in *n*-hexane. This means that the contribution of E^* to $\Delta A_\lambda(t)$ at these wavelengths is negligible compared to contributions from other types of species. Obviously, these strong absorptions in this region must be attributed to Z^*. Disregarding $\lambda = 640$ nm and $\lambda = 660$ nm, the largest value of k_1 is found at 620 nm (0.19×10^{12} s^{-1}), within the band ΔA_Z, arising from Z^*. This value is nearly 3 times larger than the values of k_1 at 480, 520, and 540 nm (0.07×10^{12} s^{-1}), which do not differ much from those found at 460 and 480 nm in the case of HMMN in *n*-hexane. The value of k_1 at 620 nm indicates a path along which Z^* is generated from its precursor at a much faster rate than is encountered in the relaxation within the band ΔA_B. This path is most likely the consequence of a ground-state equilibrium between the bare form of E and a complex $\{E,S\}$ of E and a solvent molecule S, which are both being excited by the pump pulse. Specific solute−solvent interactions have previously been shown to affect the spectral location of the fluorescence bands of HMMN in hydrogen-bonding solvents.[5] The new aspect is that these specific interactions already exist when HMMN is in its ground state.

The growth component at $580 \leq \lambda \leq 620$ nm can be attributed to a conversion of $\{E^*,S\}$ into $\{Z^*,S\}$ which is much faster than the vibrational relaxation of E^* in *n*-hexane. Because the bare form E^* must also exhibit absorptions in the red part of the spectrum, the absorptions in the range $680 \leq \lambda \leq 720$ nm (band ΔA_R) are expected to show a decay with $k_1 \approx 0.07 \times 10^{12}$ s^{-1}, at least if E^* is dominating $\Delta A_\lambda(t)$ there. Since a decay with $k_1 = 0.13 \times 10^{12}$ s^{-1} (equal to the value of k_1 in the growth at 580 nm) is observed at 720 nm, the absorption at this wavelength must be dominated by $\{E^*,S\}$. The absorptions in

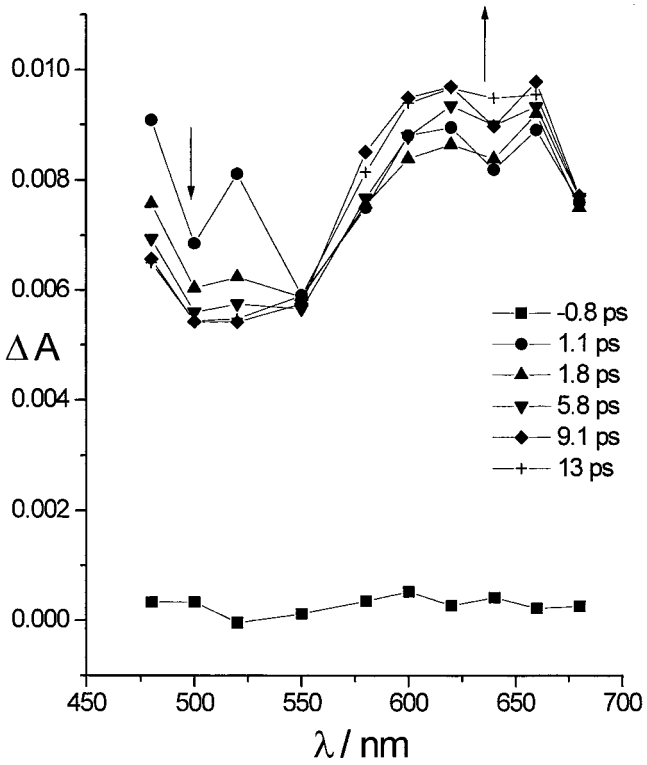

Figure 7. Evolution of the transient absorption spectrum of the solution of HMMN in 1,4-dioxane.

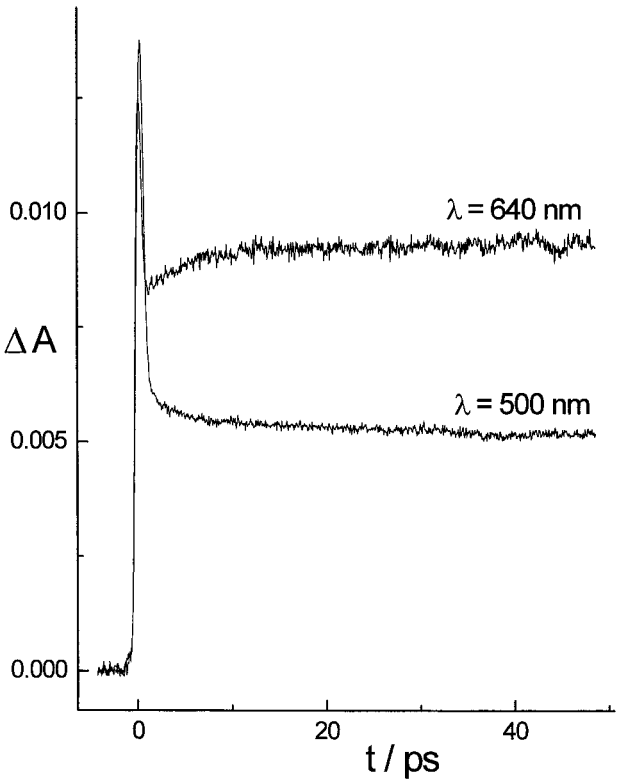

Figure 8. Time dependence of the transient absorptions of the solution of HMMN in 1,4-dioxane at 500 and 640 nm.

the red arising from $\{E^*,S\}$ are denoted as ΔA_{RS} to distinguish them from those in the red band ΔA_R of the solution in *n*-hexane. The complexes $\{E,S\}$ and $\{E^*,S\}$ must be considered to have the proton of the OH group participating simultaneously in two hydrogen bonds, one an intramolecular H-bond with the N atom in the morpholino group and the other an intermolecular H-bond with *S*. The particular role of such complexes in photoinduced proton-transfer processes has been demonstrated in the case of HMMQ.[6]

As mentioned above, forms involving E^* and Z^* are being interconverted with rate constants larger than k_L. The conversion of bare E^* into Z^* does not seem to involve $\{E^*,S\}$ as an intermediate in the time range covered, because in that case the decay of ΔA_B (i.e., $480 \leq \lambda < 560$ nm) would have to match the decay at 720 nm. The interconversion must be direct and about as fast as the vibrational relaxation of E^*.

3. Solution of HMMN in 1,4-Dioxane. ***3.a. Features of the Transient Absorption Spectrum.*** Figure 7 shows the evolution of $\Delta A_t(\lambda)$ with time in the case of the solution of HMMN in 1,4-dioxane. At time $t = -0.5$ ps, when the pump process has already been terminated, there are, in contrast to the case of HMMN in tetrahydrofurane, barely any features visible of the bands ΔA_B and ΔA_R attributed to E^* in the case of HMMN in *n*-hexane. However, at that time the features of the band arising from Z^*, i.e., ΔA_Z, are already clearly observable in the region $550 \leq \lambda \leq 620$ nm, as in the case of HMMN in tetrahydrofurane.

A rather large increase in $\Delta A_t(\lambda)$ appears throughout the whole wavelength region in the period $-0.5 < t \leq 1.1$ ps. It is followed by a decrease below 550 nm and a further increase between 550 and 680 nm. The band which has then developed in the latter region is much broader than the band in the same region, in the case of the solution in tetrahydrofurane. This broad band can be considered as the superposition of the bands ΔA_Z and ΔA_{RS}, which are closer together in the present case.

TABLE 3: Kinetic Parameters for HMMN in 1,4-Dioxane

λ [nm]	$10^3\, a_1$	k_1 [10^{12} s^{-1}]	$10^3\, a_L$	k_L [10^9 s^{-1}]
480	1.92 ± 0.05	0.33 ± 0.01	5.75 ± 0.01	0.34 ± 0
500	0.71 ± 0.08	0.16 ± 0.03	4.80 ± 0.02	0.34 ± 0
520	1.8 ± 0.1	0.64 ± 0.06	5.02 ± 0.01	0.34 ± 0
550	-0.61 ± 0.05	0.25 ± 0.03	5.42 ± 0.01	0.34 ± 0
580	-2.23 ± 0.09	0.19 ± 0.01	8.11 ± 0.02	0.34 ± 0
600	-2.65 ± 0.08	0.18 ± 0.01	9.51 ± 0.01	0.34 ± 0
620	-1.91 ± 0.05	0.19 ± 0.01	9.45 ± 0.01	0.34 ± 0
640	-1.32 ± 0.05	0.18 ± 0.01	8.91 ± 0.01	0.34 ± 0
660	-9 ± 20	1.61 ± 0.05	9.08 ± 0.01	0.34 ± 0
680	-0.9 ± 0.2	1.0 ± 0.2	7.45 ± 0.01	0.34 ± 0

3.b. Time Dependence of the Transient Absorptions. In the solutions of HMMN in 1,4-dioxane, the signals $\Delta A_\lambda(t)$ have a TPA contribution from the solvent for all the probe wavelengths. Figure 8 shows the large contributions from TPA at 500 and 640 nm, which appear as a sharp peak at the beginning. After the contribution from TPA is eliminated in the signals, the resulting $\Delta A_\lambda(t)$'s are represented as a sum of exponential functions (Table 3).

Whereas two exponential functions were needed to represent the fast component in the kinetics at the blue part of the spectrum in the two previous cases, a single exponential is now sufficient throughout the whole wavelength region. This means that the difference between k_1 and k_2 is not large enough to be distinguished kinetically when several species contribute to ΔA_λ. An average value of k_1 and k_2 then emerges in a single-exponential function for the fast kinetics. Such a situation becomes even worse when one of the species is dominating ΔA_λ in the region, as may happen when either bare *E* or complexes $\{E,S\}$ are predominantly excited by the pump pulse as a consequence of a larger extinction coefficient. The absorptions by $E^*(S_2)$, $E^*(S_1)$, $\{E^*(S_1),S\}$, and $\{E^*(S_2),S\}$ may overlap in the blue part of the spectrum, i.e., $\lambda \leq 520$ nm, and this must be considered to be the reason for the variation of k_1 in the band ΔA_B.

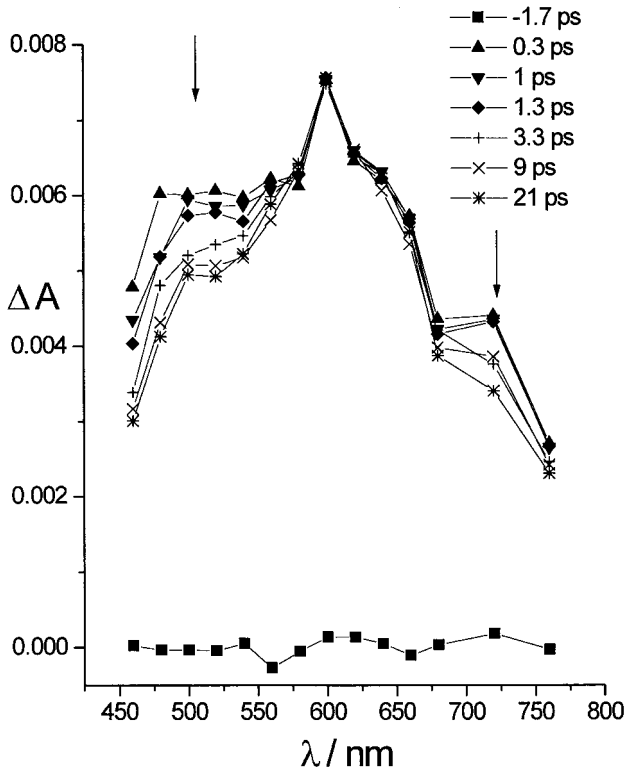

Figure 9. Evolution of the transient absorption spectrum of the solution of HMMN in acetonitrile.

In the range $550 \leq \lambda \leq 640$ nm ΔA_λ is growing with rate constant k_1, which has a constant value of about 0.19×10^{12} s^{-1} in this range. This value may be interpreted as the magnitude of the rate constant for the conversion of $\{E^*(S_1),S\}$ into $\{Z^*,S\}$, and it implies that this process is as fast as in the case of the solution in tetrahydrofurane. The largest value of k_1 is 1.61×10^{12} s^{-1}. This value is accompanied by an unreliable value of a_1 and is found in the growth of ΔA_{660}, which is not followed by a fast decay. At 680 nm the representation is more reliable and indicates a single component in the fast kinetics, which grows with $k_1 = 1.0 \times 10^{12}$ s^{-1} and has an error of about 20% in a_1. The growth of a contribution ΔA_{RS} from $\{E^*(S_1),S\}$ to ΔA_λ in the range $\lambda \geq 660$ nm is expected to be followed by a relatively fast decay associated with the conversion of $\{E^*(S_1),S\}$ into $\{Z^*,S\}$. Therefore, ΔA_λ in the range $\lambda \geq 660$ nm must be attributed to the absorption band ΔA_R of bare E^*, and one must attribute k_1 at 680 nm to the relaxation of $E^*(S_2)$ into $E^*(S_1)$ and conclude that $E^*(S_1)$ does not get converted into Z^*.

4. Solution of HMMN in Acetonitrile. ***4.a. Features of the Transient Absorptions.*** Figure 9 shows that in the whole wavelength region, the intensity of $\Delta A_t(\lambda)$ is growing only before $t = 0.3$ ps, in the case of the solution of HMMN in acetonitrile. Thereafter, ΔA_λ does not change anymore in the region $620 \leq \lambda \leq 640$ nm, although decay can then be observed clearly at all other wavelengths. Both the height and the position of the maximum at 620 nm remain fixed from $t = 0.3$ ps on. This maximum appears in the same region as the maximum of the band attributed to the complex $\{Z^*,S\}$ in the case of the solution in tetrahydrofuran; therefore, it too must be attributed to such a complex in the present case. Note, however, the striking difference between the time dependencies of this band in the two cases. The quasistationary character of the band in the present case means that the band is affected neither by vibrational relaxation nor by relaxation of the dielectric polarization of the solvent, because these effects would extend beyond $t = 0.3$ ps. Taking into account the conclusion that the bare form E^* does not get converted into a zwitterion in the solution in 1,4-dioxane, one may conclude that solvent dielectric polarization is of no significance in promoting the intramolecular proton transfer compared to the specific solute−solvent interaction in the complex $\{E^*,S\}$.

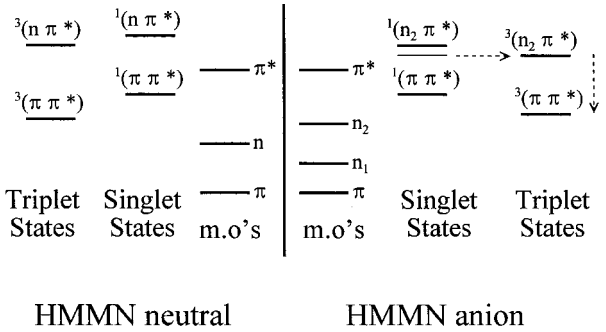

Figure 10. Expected ordering of molecular orbital levels and electronic state levels of HMMN and its anion.

In contrast to the central band in the region $620 \leq \lambda \leq 640$ nm, the absorptions at both the blue and the red side of the region are time-dependent beyond $t = 0.3$ ps. This means that the species causing these absorptions are kinetically disconnected from $\{Z^*,CH_3CN\}$ as soon as their common source has been exhausted. The absorptions at the blue and red sides of the region $620 \leq \lambda \leq 640$ nm are arising from a single type of species, because the kinetic behavior is the same at both sides. This species is most probably a species in an electronic triplet state. Taking into account that triplet states have not been emerging from either E^* or $\{E^*,S\}$ in the case of solutions in *n*-hexane, tetrahydrofurane, and 1,4-dioxane, the absorptions at the red and blue sides of the central band of the solution in acetonitrile are attributed to triplet states $^3\{Z^*,CH_3CN\}$ of the complex of Z^* with CH_3CN, which are still relaxing into the vibrationless lowest triplet state $^3\{Z^*,CH_3CN\}_1$. The reasons for invoking triplet states above $^3\{Z^*,CH_3CN\}_1$ are that no photodecomposition is involved and that a relaxed triplet state in acetonitrile has a decay rate constant of about 4.3×10^6 s^{-1} when it decays predominantly as the result of quenching by dissolved oxygen,[14] while the observed spectral changes proceed in the picosecond time domain. Apparently, spin−orbit coupling is stronger between a generated singlet state $^1\{Z^*,S\}_X$ above the vibrationless first excited singlet $^1\{Z^*,S\}_1$ state and the manifold of $^3\{Z^*,S\}$ states when S is a CH_3CN molecule than when S is a *tetrahydrofurane* or *1,4-dioxane* molecule. The state $^1\{Z^*,S\}_X$ is the common source for producing $^1\{Z^*,S\}_1$ and triplet states $^3\{Z^*,S\}$. There is no knowledge available which enables us to choose between a vibrationally excited substate of $^1\{Z^*,S\}_1$ and the second excited electronic singlet state $^1\{Z^*,S\}_2$ for the identification of $^1\{Z^*,S\}_X$. Among the solvent molecules just mentioned, CH_3CN makes the weakest H-bond[15] with the O atom of the naphtholate ion in Z^*. Efficient spin−orbit coupling requires coupling of the lowest $^1(\pi\pi^*)$ state of the naphtholate ion in Z^* to one of its $^3(n\pi^*)$ states, and this depends strongly on the energy gap between these states. The smallest energy gap and strongest spin−orbit coupling are to be expected when S is a CH_3CN molecule. This reasoning is supported by the ordering of molecular orbitals (MOs) and electronic-state energies presented in Figure 10. The levels π and π^* in this scheme refer to the highest occupied and lowest unoccupied π-type MOs, respectively, and level n refers to the MO available for the pair of nonbonding electrons on the O atom of the OH group in neutral HMMN. Two pairs of nonbonding electrons of the deprotonated O atom in the anion of HMMN occupy MOs n_1 and n_2, which are linear combina-

TABLE 4: Kinetic Parameters for HMMN in Acetonitrile

λ [nm]	$10^3\ a_1$	k_1 [10^{12} s^{-1}]	$10^3\ a_2$	k_2 [10^{12} s^{-1}]	$10^3\ a_3$	k_3 [10^{12} s^{-1}]	$10^3\ a_L$	k_L [10^9 s^{-1}]
480	0.49 ± 0.05	0.08 ± 0.03	−13 ± 35	1.6 ± 0.8	12 ± 35	1.1 ± 0.5	4.25 ± 0.05	0.26 ± 0
500	3 ± 20	0.003 ± 0.028	−9 ± 5	2.2 ± 0.2	4 ± 1	0.69 ± 0.08	2.2 ± 20	0.26 ± 0
520	0.46 ± 0.07	0.10 ± 0.03	−21 ± 135	1.5 ± 1.0	18 ± 134	1.2 ± 0.95	4.99 ± 0.03	0.26 ± 0
540	0.3 ± 0.1	0.12 ± 0.06	−15 ± 73	1.5 ± 1.0	11 ± 72	1.1 ± 1.0	5.25 ± 0.02	0.26 ± 0
560	1.4 ± 1.0	0.6 ± 0.2	−18 ± 2550	2 ± 125	12 ± 2550	2 ± 165	5.91 ± 0.01	0.26 ± 0
580	−0.39 ± 0.02	0.054 ± 0.008	−23 ± 59	3.7 ± 1.2	21 ± 59	5.0 ± 2.6	6.61 ± 0.02	0.26 ± 0
600	−2 ± 16	0.003 ± 0.022	−7 ± 6	2.38 ± 0.05			9.66 ± 16	0.26 ± 0
620	−9 ± 281	0.001 ± 0.028	−12 ± 35	1.6 ± 0.9	7 ± 35	1.2 ± 1.0	16 ± 281	0.26 ± 0
640	−0.22 ± 0.04	0.05 ± 0.03	−30 ± 400	1.5 ± 1.3	24 ± 400	1.3 ± 1.4	6.32 ± 0.05	0.26 ± 0
660	0.8 ± 0.3	0.49 ± 0.11	−11 ± 14	3.5 ± 1.6	9 ± 14	8 ± 13	5.44 ± 0.01	0.26 ± 0
680	1.0 ± 1.4	0.01 ± 0.02	−10 ± 23	1.5 ± 0.6	6 ± 20	1.0 ± 0.6	3 ± 1	0.26 ± 0
720	0.6 ± 0.09	0.09 ± 0.02	−7 ± 11	2.1 ± 0.4	3 ± 3	0.9 ± 0.3	3.56 ± 0.03	0.26 ± 0
760	0.62 ± 0.08	0.36 ± 0.04	−3.1 ± 0.5	2.3 ± 0.1			2.4 ± 0.3	0.26 ± 0

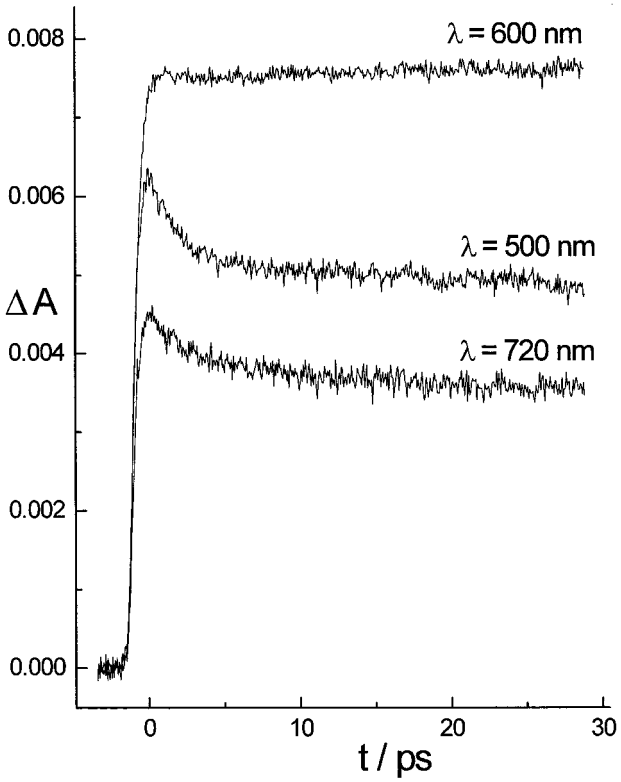

Figure 11. Time dependence of the transient absorptions of the solution of HMMN in acetonitrile at 500, 600, and 720 nm.

tions of the degenerate sp^2 hybrid atomic orbitals of this atom. The strong fluorescence from all forms of HMMN indicates that their lowest excited singlet state is a $^1(\pi\pi^*)$ state. Because MO n_2 lies above MO n, the energy gap between states $^1(n_2\ \pi^*)$ or $^3(n_2\ \pi^*)$ and state $^1(\pi\pi^*)$ is smaller than the gap between states $^1(n\ \pi^*)$ or $^3(n\ \pi^*)$ and $^1(\pi\pi^*)$.

4.b. Time Dependence of the Transient Absorptions. In this particular case, the time dependence of the depolarization of the transient absorption has been studied over a range of 30 ps at two wavelengths, by detection with probing light polarized either parallel or perpendicular to the polarization of the pumping light. The initial anisotropies of the transient absorptions at 480 and 600 nm have been found to decay with a common time constant of about 20 ps. The magnitude of this time constant indicates that the depolarization is caused not by fast intramolecular processes, but by overall rotation of the excited solute. The time dependence of $\Delta A_\lambda(t)$ of the solution of HMMN in acetonitrile is shown in Figure 11 for $\lambda = 500$, 600, and 720 nm. No TPA contributions from the solvent are observed in this case. The absorption at 600 nm is generated within the period of laser excitation and remains constant thereafter in the time range covered.

The representation of the time dependence of $\Delta A_\lambda(t)$ as a sum of exponential functions has not been as successful as in the previous cases (Table 4). The result is not satisfactory at several wavelengths with either two or three exponential functions in the representation of the fast kinetics. Based on the assignment of the blue and red part of the spectrum to absorptions by the lowest $^3\{Z^*,S\}$, this is not surprising, because in addition to the fixed value of k_L for the decay of the $^1\{Z^*,CH_3CN\}_1$ state, the decay rate constant k_T for the decay of $^3\{Z^*,CH_3CN\}_1$ must be introduced and assigned a fixed value. This has not been done, because the fitted functions would not have been trustworthy when at least six adjustable parameters (two rate constants and four pre-exponential coefficients) were involved.

5. Solution of HMMQ in Tetrahydrofurane. ***5.a. Features of the Transient Absorption Spectrum.*** Acetonitrile was not chosen as solvent for HMMQ so that we might avoid the formation of triplet states which occurred in the case of the solution of HMMN. Tetrahydrofurane was preferred over 1,4-dioxane as solvent for HMMQ, because the excited keto form of HMMQ emerges in much higher yield when tetrahydrofurane is used. The evolution of $\Delta A_t(\lambda)$ of HMMQ in tetrahydrofurane during the first 45 ps after laser pulse excitation is presented in Figure 12. To assign the absorptions in the various regions of the spectrum, it is useful to bear in mind that photoexcitation of solutions of the enol form *E* of HMMQ in tetrahydrofurane leads to fluorescence from excited zwitterionic forms between 400 and 500 nm and fluorescence from the excited keto form between 545 and 670 nm.[5] Recall also that the first UV−visible absorption band of the ground-state keto tautomer of 7-hydroxyquinoline in 2-propanol has its maximum at 420 nm.[2] The ground-state keto form of HMMQ may therefore be expected to have its first UV−visible absorption band in the same wavelength region, because the chromophoric system is the same.

For $\lambda < 500$ nm, the intensity is negative in the beginning because of the contribution of stimulated emission. At time $t =$ 0.8 ps, the spectrum is broad and rather featureless, with a not very pronounced maximum in the intensity around 600 nm. This observation is in contrast with the relatively sharp band around 640 nm, attributed to *Z** type species, in the case of the solution of HMMN in tetrahydrofurane. The difference may be attributed to a rigid structure of *Z**, kept fixed by intramolecular H-bonding, in the latter case and a protonated morpholino group in the *Z** form of HMMQ which is subjected to rotational Brownian motion. The various positions taken by the proton on the morpholino group relative to the electronically excited aromatic moiety in HMMQ yield different spectra and cause spectral broadening, due to variation of the interaction between

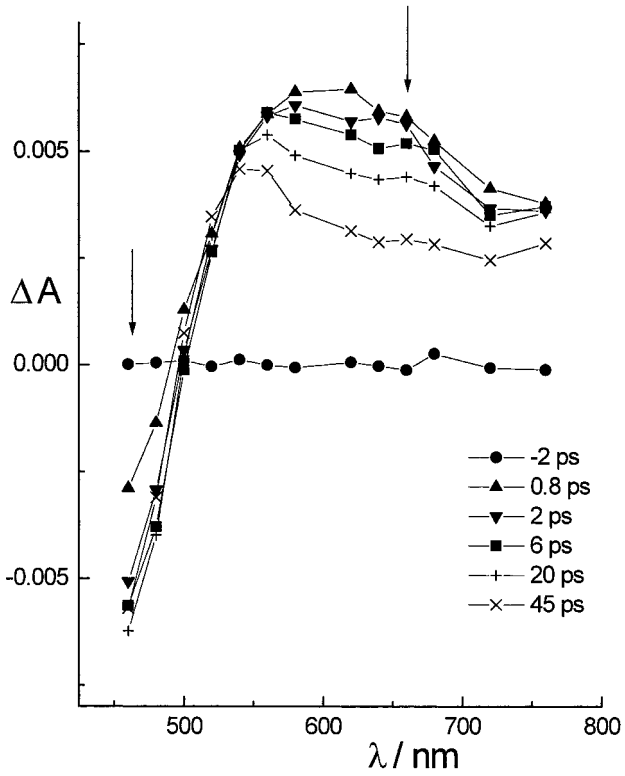

Figure 12. Evolution of the transient absorption spectrum of the solution of HMMQ in tetrahydrofurane.

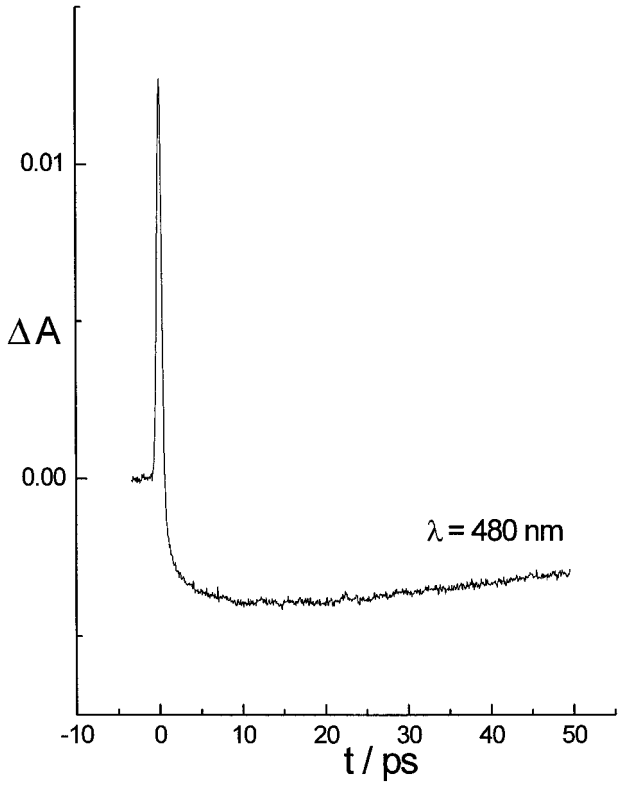

Figure 13. Time dependence of the transient absorptions of the solution of HMMQ in tetrahydrofurane at 480 nm.

the two subsystems. The observed broadening provides experimental support for the procedure, introduced in simulations of the photoinduced tautomerization of HMMQ, in which the electron distribution of the excited chromophoric part of the molecule is adapted to the position of the protonated morpholino group.[7,16] As time proceeds the spectrum sharpens gradually, and at $t = 45$ ps a narrower band can be seen around 550 nm. The sharpening can be attributed to the buildup of the keto form *K**, whose spectrum is not expected to be strongly dependent on the position of the morpholino group, because the two interaction subsystems are now electrically neutral.

5.b. Time Dependence of the Transient Absorptions. Figure 13 shows a typical time dependence of the transient absorptions of a solution of HMMQ in tetrahydrofurane for the probing wavelength of 480 nm. The sharp peak at the beginning of the signal arises from two-photon absorption by the solvent. Immediately after this peak disappears, the signal starts to become negative in contrast to the solution of HMMN in tetrahydrofurane.The reason for this behavior is that both transient absorption by and stimulated emission from the *Z** form of HMMQ are contributing to the signal. This did not happen in the case of HMMN in tetrahydrofurane, because the fluorescence band of the *Z** form of HMMN is much more to the blue, i.e., outside the region of the probing wavelengths. The figure offers no sign of the conversion of *E** into a *Z**, even after numerical elimination of the TPA contribution. This means that the former process is too fast to be resolved with the available time resolution. The figure reveals clearly that a relaxation process is proceeding on a time scale extending beyond 50 ps. This process can be observed in the whole visible part of the spectrum, but it is seen most clearly at wavelengths below 500 nm. Its time dependence is displayed on a much longer time scale in Figure 14, where the induced absorptions at 460 and 600 nm are shown together as a function of time. This figure shows clearly that in the time interval $0 < t < 375$ ps, the stimulated emission at 460 nm (from {*Z**,*S*}) is decaying

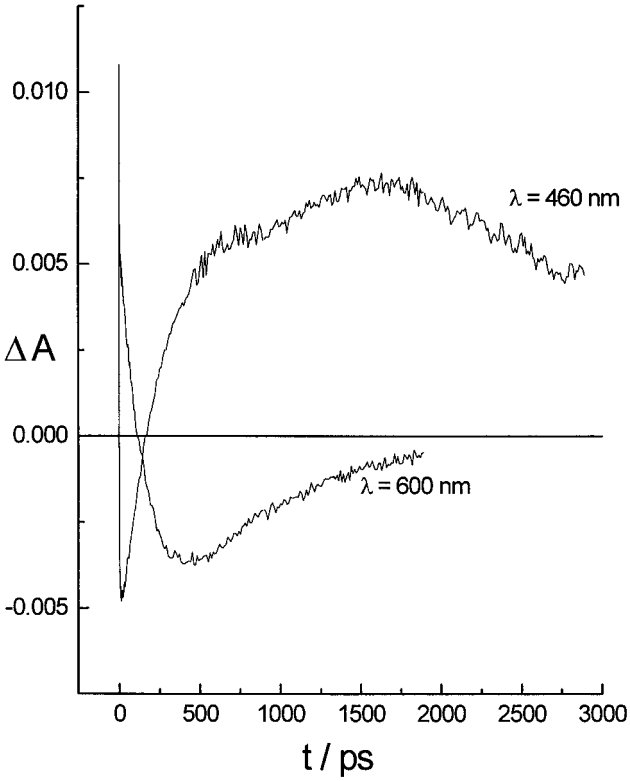

Figure 14. Time dependence of the transient absorptions of the solution of HMMQ in tetrahydrofurane at 460 and 600 nm.

with a rate constant k_r equal to the one involved in the growth of the stimulated emission at 600 nm (from {*K**,*S*}). This observation reflects the conversion of the zwitterionic form *Z** of HMMQ into its keto form *K** resulting from the rotational Brownian motion of the protonated morpholino group. The

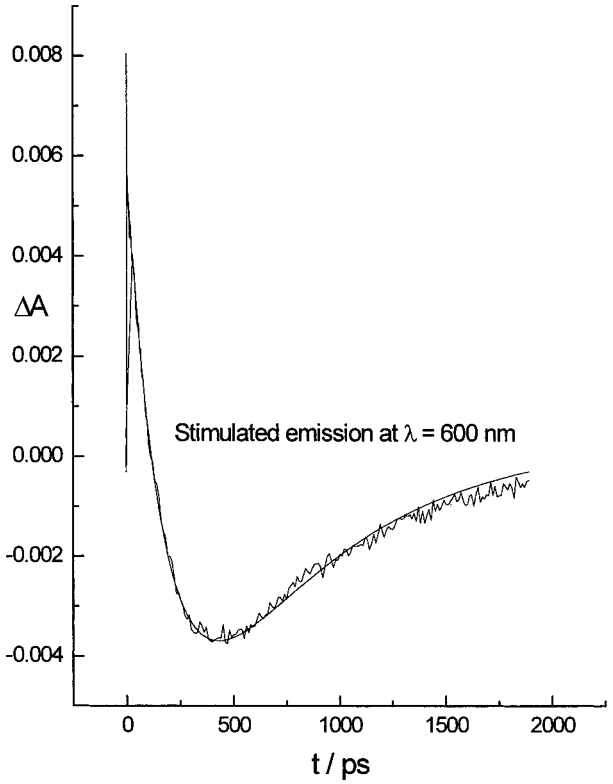

Figure 15. Experimental and fitted time dependence of the transient absorption of the solution of HMMQ in tetrahydrofurane at 600 nm.

signal at 600 nm in the figure starts to decay (*mono*exponentially) around $t = 375$ ps and continues to do so, with rate constant k_d, until it has disappeared at about $t = 2000$ ps, while the signal at 460 nm grows at the same rate in the time elapsed between these instants. This reflects the conversion of the excited K^* form to ground-state keto form K along radiative and radiationless pathways. Because $\Delta A_{600}(t)$ contains only contributions with the rate constants k_r and k_d, the values of these rate constants can be estimated by fitting a *bi*exponential function to them. The fit shown in Figure 15 yields $k_r = 5.6 \times 10^9\ s^{-1} \pm 1\%$ and $k_d = 1.4 \times 10^9\ s^{-1} \pm 2\%$. This value for k_d is equal to the one reported for a solution of HMMQ in 1,4-dioxane.[11] The signal at 460 nm starts to decay around $t = 2000$ ps, with rate constant k_t, and continues to do so beyond $t = 3000$ ps. The latter behavior reflects the ground-state *re*tautomerization, which leads from the ground-state keto form K to the ground-state enol form E of HMMQ. The value of k_t cannot be determined accurately, because the time range covered is short compared to k_t^{-1}. However, a reasonable estimate can be made, and this yields $k_t \approx 0.3 \times 10^9\ s^{-1}$.

6. Conclusion

In the systems HMMN and HMMQ, excited 2-naphthol is a weaker proton donor compared to excited 7-hydroxyquinoline, this weakness slowed the proton transfer to the morpholino group considerably and enabled the observation of several processes preceding ESIPT in HMMN. Previously, attention has been drawn to the advantages HMMQ offers in the experimental study of the influence of solvent-imposed friction on the motion of reactants in liquid solutions. Until now, comparison between experiment and theory has had to be restricted to the rotational Brownian motion of the protonated morpholino group in excited HMMQ. Such a process can now be observed in the case of a ground-state molecule, namely the ground-state keto form of HMMQ. This work opens the field for further experimental studies on the influence of solvent-imposed friction on the *re*tautomerization of keto−HMMQ in its ground state. The comparison between experiment and theory or simulation can then be performed in a more reliable manner, because the solute−solvent interactions can be calculated quite easily in the case of the ground-state solute. Note that the ground state *re*tautomerization of HMMQ starts within a few nanoseconds after the excited state of the enol form has been prepared.

References and Notes

(1) Konijnenberg, J.; Huizer, A. H.; Varma, C. A. G. O. *J. Chem. Soc., Faraday Trans. 2* **1988**, *84*, 1163.

(2) Konijnenberg, J.; Ekelmans, G. B.; Huizer, A. H.; Varma, C. A. G. O. *J. Chem. Soc., Faraday Trans. 2* **1989**, *85*, 39.

(3) Köhler, G.; Wolschann, P. *J. Chem. Soc., Faraday Trans. 2* **1987**, *83*, 513.

(4) Eisenthal, K. B. In *Ultrashort Laser Pulses*; Kaiser, W., Ed.; Springer-Verlag: Berlin, 1988.

(5) Jalink, C. J.; Van Ingen, W. M.; Huizer, A. H.; Varma, C. A. G. O. *J. Chem. Soc., Faraday Trans.* **1991**, *87*, 1103.

(6) Davydov, A. S. *Solitons in Molecular Systems*; D. Reidel Publishing Company: Dordrecht, The Netherlands, 1984.

(7) Jalink, C. J.; Huizer, A. H.; Varma, C. A. G. O. *J. Chem. Soc., Faraday Trans.* **1992**, *88*, 1643.

(8) Jalink, C. J.; Huizer, A. H.; Varma, C. A. G. O. *J. Chem. Soc., Faraday Trans.* **1992**, *88*, 2655.

(9) Jalink, C. J.; Huizer, A. H.; Varma, C. A. G. O. *J. Chem. Soc., Faraday Trans.* **1993**, *89*, 1677.

(10) Geerlings, J. D.; Huizer, A. H.; Varma, C. A. G. O. *J. Chem. Soc., Faraday Trans.* **1997**, *93*, 237.

(11) Geerlings, J. D.; Varma, C. A. G. O. *J. Photochem. Photobiol., A* **1999**, *129*, 129.

(12) de Bekker, E. J. A.; Geerlings, J. D.; Varma, C. A. G. O. *J. Phys. Chem. A* **2000**, *104*, 5916.

(13) Reuther, A.; Laubereau, A.; Nikogosyan, D. N. *Opt. Commun.* **1997**, *141*, 180.

(14) van Eijk, A. M. J.; Verhey, P. F. A.; Huizer, A. H.; Varma, C. A. G. O. *J. Am. Chem. Soc.* **1987**, *109*, 6635.

(15) Goldman, M.; Wehry, E. L. *Anal. Chem.* **1970**, *42*, 1178.

(16) Geerlings, J. D.; Varma, C. A. G. O.; van Hemert, M. C. *J. Phys. Chem A.* **2000**, *104*, 7409.